Reinforcement Mechanism of Nanofilled Polymer Melts As Elucidated by Nonlinear Viscoelastic Behavior

S. S. Sternstein* and Ai-Jun Zhu

Materials Science and Engineering Department, Rensselaer Polytechnic Institute, Troy, New York 12180

Received March 27, 2002

ABSTRACT: Nonlinear viscoelastic properties are reported for composites of fumed silica with various surface treatments and matrices of poly(vinyl acetate) of different molecular weights as well as a copolymer matrix of vinyl acetate and vinyl alcohol. Data above the glass transition temperature are reported here. The increase in the composite storage and loss moduli measured at low strains, and their relative rates of decrease with strain, are found to depend on filler surface treatment. The nonlinear behavior of the loss factor with strain is dramatically altered by filler treatment and quite revealing as to the likely mechanism causing the nonlinearity. In addition, the relative reinforcement and the degree of nonlinearity are found to be the highest for the lowest molecular weight matrices. The effect of copolymer substitution for the homopolymer matrix is equivalent to an increase in molecular weight. The primary underlying mechanism for reinforcement and nonlinear behavior appears to be the filler−matrix interactions, but not filler agglomeration or percolation. It is proposed that temporary (labile) bonding of chains to the filler surface results in trapped entanglements, having both near- and far-field effects on matrix chain motions. These trapped entanglements cause greatly enhanced non-Gaussian (Langevin) chain behavior that affects storage and loss moduli differently, resulting in very high reinforcement by nanofillers. Applied strain (stress) aids the release of the trapped entanglements, thereby leading to the reduction in dynamic moduli. The reinforcement and nonlinear viscoelastic properties of the nanofilled polymer melts bear striking similarity to what is observed in filled elastomers (the Payne effect), suggesting a common mechanism that is rooted in the macromolecular nature of the matrices.

Introduction

The nonlinear dynamic mechanical properties of elastomers filled with carbon black were investigated by Payne[1] nearly 40 years ago, but the mechanisms for reinforcement and nonlinearity remain controversial. A widely held view is that filler agglomeration and network formation are responsible for the high levels of reinforcement and that deagglomeration and network breakdown are responsible for the nonlinearity with strain.[2,3] There is substantial evidence to suggest that agglomeration and percolation do occur in filled elastomers and that the filler structures are highly dependent on the particular filler and the mixing method used for composite preparation. However, many studies on filler-structure effects are typically carried out at high volume fractions of filler. There is relatively little information regarding nonlinear viscoelastic behavior at low filler contents, particularly below the percolation threshold.

As normally defined, the Payne effect in filled elastomers refers to the reduction of dynamic storage modulus with increasing strain amplitude. This nonlinearity is absent in the neat elastomers when tested at the same strain levels. Maier and Goritz[4] have proposed an alternative mechanism to filler-structure breakdown suggesting that the Payne effect is due to the stress-induced debonding of polymer chains from the filler surface. These authors provide a simple set of equations to account for the decrease of storage and loss moduli with strain in filled elastomers, but the theory fails to account for many rheological features that go hand in hand with the Payne effect. Filler-structure-based theories and the debonding theory are difficult to distinguish experimentally since filler−filler and filler−matrix interactions are both dependent on specific filler characteristics such as surface treatment.

Recently, Chazeau, Brown, Yanyo, and Sternstein[5] have reported a number of phenomena that are directly related to the Payne effect. Briefly, these authors find that a wide variety of filled elastomers share a number of generic nonlinear features as observed in simple shear. (1) Dynamic storage and loss moduli measured on fully equilibrated samples are dependent on the dynamic strains only and independent of a simultaneous (fully equilibrated) static strain. (2) Stress−strain curves obtained at constant strain rate give an initial to terminal modulus ratio that is nearly the same as the ratio of the dynamic storage moduli obtained at low and high strains, respectively. (3) The incremental stress−strain curves are also independent of a fully equilibrated static strain. (4) The initial modulus in the constant strain rate test is highly rate dependent whereas the terminal modulus is constant with strain rate. Extrapolation of the results suggests that the initial and terminal moduli would be equal at a strain rate of about 1.0×10^{-7} per second. Equivalently, this suggests that the Payne effect observed in a dynamic test would vanish at frequencies below about 1.6×10^{-5} Hz. (5) Large-strain perturbations, such as the imposition of a static strain, removal of a static strain, or a large-amplitude dynamic strain, all result in a subsequent reduction of the storage modulus at low strain that is fully recoverable with time to its preperturbation value. Furthermore, the recovery kinetics is essentially independent of the nature of the large perturbation.

Taken together, these observations show that the Payne effect is dependent on the dynamic (time varying) strain only, which suggests that the nonlinear viscoelastic behavior due to filler addition is viscously (rather than elastically) coupled to the applied strain. This conclusion has major ramifications regarding the underlying mechanism responsible for the Payne effect and

10.1021/ma020482u CCC: $22.00
Published on Web 08/09/2002

its modeling. In this regard, the nonlinear viscoelastic behavior of filled (but un-cross-linked) polymer melts is highly relevant and provides the stimulus for the present investigation.

Cross-linked elastomers and un-cross-linked polymer melts display similar filler effects on dynamic mechanical properties. For polymer melts the strain amplitude corresponding to the onset of nonlinear behavior is also reduced by the addition of filler,[6] which is similar to the Payne effect. Micron-sized and smaller fillers in melts greatly increase the dynamic moduli[7,8] as they do in cross-linked elastomers. However, it is well-known that this high reinforcement in storage modulus is often far larger than can be explained by simple micromechanical mixing analysis. This is true even for low filler concentrations, which strongly implies that interparticle stress−field interactions are not the source of the high reinforcement. Damping in filled elastomers is generally increased by the addition of filler. Similarly, damping in filled polymer melts has been reported to increase.[9,10] However, as the present study shows, the loss factor behavior in polymer melts is more complicated and may either increase or decrease with filler addition, depending on the filler surface treatment and the strain amplitude and history.

Filler size effects are observed in both filled elastomers[7,11] and filled polymer melts,[12−14] but the mechanisms are not fully understood. Micromechanical treatments do not predict an intrinsic size effect, the volume fraction being the only relevant variable at low filler concentrations. There is a tendency for the fillers to form some sort of "weak structure" when filler size becomes very small, although the exact nature of this structure is not clear. It is also difficult to separate a true size effect from agglomeration. Some workers tend to equate "microstructure" to "agglomeration" or filler networking,[13,15] and therefore filler agglomeration is also widely cited for the nonlinear behavior of filled polymer melts. Although filler size affects the tendency to agglomerate, the present results suggest an alternative theory for the size effect on filled polymer behavior.

Filler network formation belongs to the family of phenomena that can be described by percolation theory. According to statistical treatments, there exists a "threshold" value for percolation to occur. For instance, it is calculated to be 31.2 vol % for the 3-dimensional simple cubic lattice model.[16] Electrical conductivity measurements on carbon-black filled natural rubber demonstrate the existence of such a threshold filler level, below which (ca. 15 vol %) the material displays conductivity values typical of unfilled rubbers and above which the conductivity increases abruptly.[17] Similarly, Gerspacher et al.[18] suggest that a critical value of carbon-black loading exists below which the contribution of filler networking to low strain mechanical behavior becomes minor, and this critical value is about 19 vol % for a specific black. The present work also suggests that neither agglomeration nor percolation is the primary factor causing the nonlinear behavior or the levels of reinforcement observed. If the high reinforcement can be explained by something other than filler agglomeration or percolation, then it follows that the drop of modulus with strain can also be explained by something other than deagglomeration or network breakdown, respectively. In addition, any viable mechanism must correspondingly explain the recovery of moduli with time following a large strain perturbation.

An often-cited experimental result given by Payne[19] is that nonpolymeric liquids such as *n*-decane and liquid paraffins display the Payne effect when filled with carbon blacks. This is taken as evidence that filler networking and/or agglomeration are responsible for the Payne effect. The lowest filler concentration used in Payne's work was 28 vol %. However, this neither proves nor disproves the converse, namely that in a polymeric melt, filler agglomeration and network formation are required to produce a Payne effect. The present work indicates that the Payne effect can occur in a polymeric melt at filler concentrations as low as 1 vol %, far below the percolation threshold and with the filler particles essentially isolated in the micromechanical sense (nonoverlapping stress fields). However, far-field filler effects do occur, but they are rooted in the macromolecular nature of the matrix itself.

If neither filler agglomeration nor network formation is a prerequisite for nonlinear behavior, then the filler−matrix interface as well as its behavior under stress is a likely alternative. In addition, the influence of the interface on far-field matrix behavior may be a significant factor in high molecular weight polymers. The bonding and debonding between polymer chains and filler surfaces and the effects on viscoelasticity have been studied and modeled.[20,21] Furthermore, recent studies on the interactions of unfilled polymer melts with flat surfaces are intriguing and may provide clues regarding the polymer−filler interactions in filled melts.

Studies on the flow of unfilled high polymers across flat surfaces are numerous since they pertain to many important topics such as adhesion and adhesive failure, friction, and flow instabilities such as melt fracture. We believe that these studies provide many insights into the behavior of filled systems as well. Recently, Leger and co-workers[22] have shown that polymers slip on a flat surface when sheared, regardless of the shear rate. Even when some polymer chains are permanently tethered to the surface, slippage occurs due to a complex disentanglement process between the tethered chains and the bulk polymer. This disentanglement develops in three regimes with respect to shear rate. At sufficiently high strain rate, the surface chains and bulk polymer are effectively disentangled and therefore dynamically decoupled. Rheological models have been proposed by Graham[23] for the slip at polymer/solid interfaces, which include the effects of drag on polymer chains, disentanglement, and detachment and reattachment of chains at the solid surface. Notwithstanding the structural complexities of a particulate filled system, it is our opinion that filled systems under stress exhibit the same phenomena as described by Leger and Graham regarding the flow of unfilled polymers over flat surfaces. The rheological results presented here can be explained in terms of the filler−matrix interactions and the manner in which these interactions are altered by the application of a shear stress and ultimately result in slip.

It was proposed many years ago that filler particles should cause an increase in the number of entanglements in filled systems.[24] Chain entanglements can alter a material's viscoelastic behavior, for example, by affecting the particle diffusivity[25] in a polymer matrix or by causing a strain dependence of dynamic modulus measured simultaneously during stress relaxation[26] in a neat polymer. Recent experiments on thin polymer films (nanoscale) confined between adsorbing surfaces

suggest that geometrical confinements enhance entanglement interactions between polymer chains even in the case of weak adsorption.[27−28] Thin polymer melts show a dramatic nonlinear response in dynamic shear experiments at large stains,[29] which is attributed to strain-induced disentanglement and the slippage of adsorbed polymer layers at the confining surfaces.

In summary, filled (cross-linked) elastomers and filled (un-cross-linked) polymer melts show similar nonlinear viscoelastic behavior with respect to both strain and filler characteristics. This similarity is due to the fact that both materials are composed of long polymer chains above the glass transition temperature, where they obey similar chain conformation statistics. In both cases, the presence of entanglements due to either topological restraints (including chemical cross-links or labile bonds to the filler surface) or specific energetic interactions (such as hydrogen bonding) is clearly a major factor controlling the viscoelastic behavior. The primary difference in rheological behavior is that the chemical cross-links restrict or eliminate the longer relaxation time processes in the matrix. It is our belief that the nonlinearity observed in filled systems, whether cross-linked or not, with the matrix above the glass transition temperature, is rooted in the nature of the polymeric matrix and the manner in which the filler−matrix interface alters matrix behavior in the presence of an applied stress. Therefore, filled elastomers and polymer melts should share a fundamental mechanism regarding the origin of the nonlinear viscoelasticity, as suggested by the present work.

Experimental Section

Composites were prepared using matrix polymers of poly(vinyl acetate) (PVAc) of 40K, 83K, and 140K weight-average molecular weights. The PVAc polymers with 83K and 140K MW were obtained from Aldrich and used as received. The 40K PVAc was obtained by mixing the 83K polymer with a 13K PVAc sample also obtained from Aldrich. A vinyl acetate/vinyl alcohol copolymer was obtained from Scientific Polymer Products, with 18% vinyl alcohol content and M_w about 92K. These polymers have glass transition temperatures in the vicinity of 43 °C measured dynamically at 2 Hz. Only the above T_g data are considered here. Fumed silicas obtained from Cabot and Aldrich were used as fillers, with specific surface areas ranging from 100 to 380 m^2/g. The fillers are either in the nontreated (NT) form or surface treated (ST) with different organic groups. The nontreated fillers have surface hydroxyl groups, which has been confirmed by our IR data. Hydroxyl groups on silica surfaces can form hydrogen bonds with the acetate group of the matrix polymer PVAc, a proton acceptor. This type of hydrogen bonding has been verified by Shang et al.[30] using diffuse reflectance infrared spectra.

As obtained from Cabot, organic groups, either simple small groups (S) or long polymeric chains (L), were chemically bonded to the filler surface to replace the hydroxyl groups (see Table 1) and make the surface hydrophobic. ST-100L is covered by covalently bonded (tethered) silicone polymer chains. ST-100S filler is only partially modified, which can be seen from its carbon content or by IR spectra. However, according to Cabot, the grafted organic groups on its surface form a dimethylsilyl structure that can partially shield adjacent hydroxyl groups from interacting with the matrix, which is substantiated by our results.

The matrix polymer was first dissolved in acetone, and the correct amount of filler powder was then blended into the solution. The mixture was stirred until apparent homogeneity was achieved, followed by ultrasonication treatment for better dispersion. After sonication, the mixture was predried in air by heating and then dried in a vacuum oven at ca. 60 °C for overnight. The dried mixture was ground into powder and redried in a vacuum. To ensure good dispersion, 25 phr (parts filler per hundred parts matrix polymer by weight, where 1 phr is approximately 0.5 vol %) was the highest filler concentration used in this work.

Table 1. Specifications of Fumed Silica Fillers

filler name	specific area (m^2/g)	diameter (nm)	surf. treat.[a]
NT-380	∼380	∼7	
NT-200	200 ± 15	∼13	
ST-200S	205−245	∼13	HMDS
NT-100	100 ± 15	∼27	
ST-100S	105−145	∼27	DMDC
ST-100L	105−130	∼27	PDMS

Surface Data on ST Fillers (*Si−O*: Silica Particle Surface)

filler name	carbon content (wt. %)	surface chemistry
ST-200S	4.25 ± 0.5	$Si-O-Si(CH_3)_3$
ST-100S	0.86 ± 0.15	$Si-O-Si(CH_3)_2-O-Si(CH_3)_2-O-Si$
ST-100L	5.4 ± 0.6	$Si-O-(Si(CH_3)_2-O)_n-Si-(CH_3)_3$

[a] HMDS = hexamethyldisilazane, DMDCS = dimethyldichlorosilane, and PDMS = poly(dimethylsiloxane).

A custom test fixture and sample-molding jig were designed for this investigation. The test fixture consisted of concentric cylinders (cup and plunger) in which the inner cylinder was coupled to a load cell and the outer cylinder coupled to the actuator of the Dynastat mechanical spectrometer used for the viscoelastic measurements. The sample-molding jig provided a convenient method to mold the composite powder into the annular gap while retaining perfect coaxial alignment of the two cylinders. Composite powder was melted and molded at around 110 °C in air. All molded samples were found to be optically clear, indicating good dispersion of the silica particles in the polymer matrix. SEM pictures of the fracture surfaces of many samples also verified that the particles are well dispersed, with good adhesion to the matrix polymer.

After molding, the test fixture was transferred to the Dynastat frame at room temperature, thereby maintaining the accurate alignment achieved during molding. The axial motion of the coaxial cylinder geometry provides essentially simple shear on the material in the annular gap, albeit with a gradient in shear strain and stress with respect to radius. Results reported in this paper correspond to values computed for the inner cylinder radius. To maintain accuracy under widely varying conditions, several test fixture sizes were fabricated. Depending on the molecular weight of the matrix, the temperature, filler content, and filler surface treatment, a particular fixture size was chosen to allow an optimum range in shear-strain amplitude values to be investigated. While relatively small due to the high stiffness of the Dynastat, corrections were still made for the machine compliance. This correction was minimal for the above T_g data reported here but significant for the glass transition data obtained using a symmetric simple-shear sandwich and reported elsewhere.[31] A range of dynamic frequencies from 0.1 to 10 Hz was investigated, and the data presented here are representative of the data at any frequency. Shear-strain amplitude was a major variable in this study and was varied from 0.0014 to 0.26 (strain sine wave amplitude, peak to center).

Results

The results on the 83K MW PVAc are presented first. All data were obtained at 90 °C, with two exceptions. The copolymer data were obtained at 95 °C and the glass transition data at about 45 °C. For convenience throughout the paper, the following abbreviations are used: LAM refers to the storage modulus measured at low-amplitude (ca. 0.0014) strains, and HAM refers to the storage modulus measured at high-amplitude (ca. 0.26) strains. LALM refers to the loss modulus measured at low-amplitude strains, and HALM refers to the loss modulus measured at high-amplitude strains.

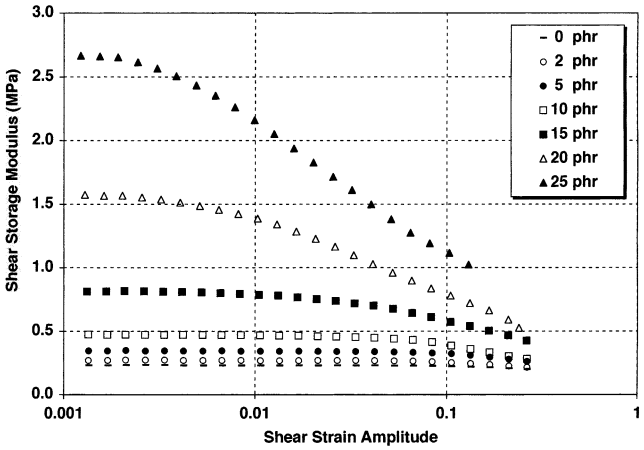

Figure 1. Shear storage modulus vs shear strain amplitude at 90 °C and 5 Hz for NT-380 silica filled 83K PVAc from 0 to 25 phr.

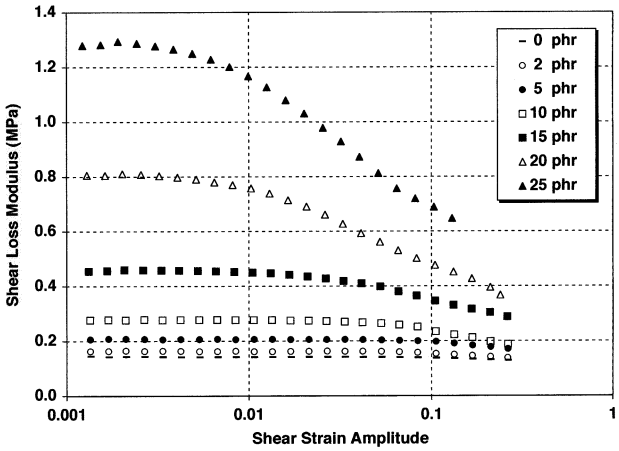

Figure 2. Shear loss modulus vs shear strain amplitude at 90 °C and 5 Hz for NT-380 silica filled 83K PVAc from 0 to 25 phr.

The effects of shear-strain amplitude on storage and loss moduli are shown in Figures 1 and 2, respectively, for the NT-380 composites at various filler concentrations and also for the neat polymer. The results are markedly similar to the behavior seen in filled elastomers.[5] The neat polymer displays linear viscoelastic behavior below about 0.10 strain. While not obvious from these graphs due to the scale used, there is a gradual reduction in both storage and loss moduli of the neat polymer for strains above 0.10, which is typical behavior for an unfilled linear high polymer.

As filler content is increased, the strain amplitude at which nonlinearity begins moves to a lower value, and for the 25 phr (12.5 vol %) sample it becomes as low as 0.002, a strain threshold that is 50 times lower than that for the neat polymer. Of more importance, however, is that the degree of nonlinearity increases continually with filler concentration, without any jump or discontinuity in behavior. This strongly suggests that filler percolation (network formation) is not a requirement for the observed nonlinear behavior. From Figure 1, the range of LAM values from neat to highly filled (25 phr) samples is substantially higher than the corresponding range of the HAM values. The highest filler concentration is substantially lower than the percolation threshold computed for most models.

Referring to Figure 1, it appears that the HAM values are converging to terminal values but that the maximum strain amplitude used here is insufficient to achieve these values. Higher strains could not be used for composites of this filler due to force limitations imposed by the apparatus and the particular sample size, stiffness, and geometry. The strain amplitude required to achieve a terminal HAM value is dependent on the particular filler surface treatment. For example, strains of 0.26 were sufficient to achieve terminal values for the ST-200S composites, as reported elsewhere.[31]

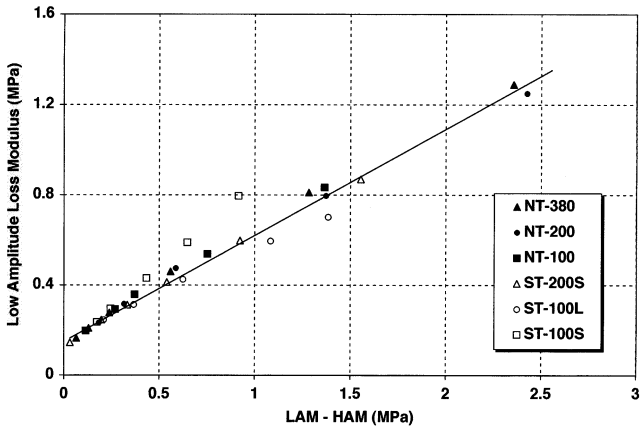

Figure 3. "Payne plot" for all 83K PVAc composites. All the silica fillers are included. LALM is the loss modulus at low strain, LAM is the storage modulus at low strain, and HAM is the storage modulus at high strain. Data were taken at 90 °C and 5 Hz.

The behavior of the loss moduli with strain and filler concentration shown in Figure 2 is essentially similar to the behavior described for the storage moduli. However, two points are worth noting. The range of the LALM with filler concentration is significantly lower than for the LAM. Also, the rate of decrease of loss modulus with strain is different than that of the storage modulus. These differences are strongly dependent on the particular filler treatment and will be illustrated in detail later in this paper.

In his study on elastomers filled with carbon black, Payne showed that the maximum value of loss modulus varies linearly with the difference between low- and high-amplitude storage moduli (in our terminology, LAM − HAM). Recently, it has been shown that Payne's observation is obeyed by a wide variety of filler types and host elastomer matrixes.[5] In the present study, for those fillers where terminal HAM values could not be directly measured, they were estimated using the equation $\mathrm{HAM} = M'(1 + 2.5\phi + 14.1\phi^2)$, where ϕ is the volume fraction of filler and M' is the storage modulus of the neat polymer measured at 0.26 strain. This equation was proposed by Guth and Gold for the dependence of storage modulus on filler content assuming limited particle−particle interactions and was found to give a reasonable estimation of terminal HAM values. From Figure 2, the maximum value of loss modulus occurs at the lowest strains, as it does for all filler-type composites investigated here. The maximum value of the loss modulus is plotted vs {LAM − HAM (estimated)} for each composite in Figure 3. With the exception of the ST-100S filled composites, which show a substantial deviation in slope, all other composites appear to lie on a single curve. Once again, this behavior is similar to the behavior of many filled elastomers.

The effect of filler concentration on the LAM values is shown in Figure 4 for composites of all six fillers. LAM increases linearly below a filler concentration that is

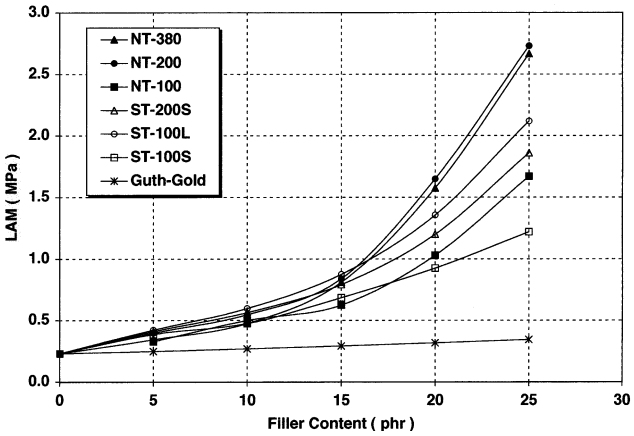

Figure 4. LAM vs filler content at 90 °C and 5 Hz for 83K PVAc composites of all silica fillers. The Guth−Gold estimation is included for comparison.

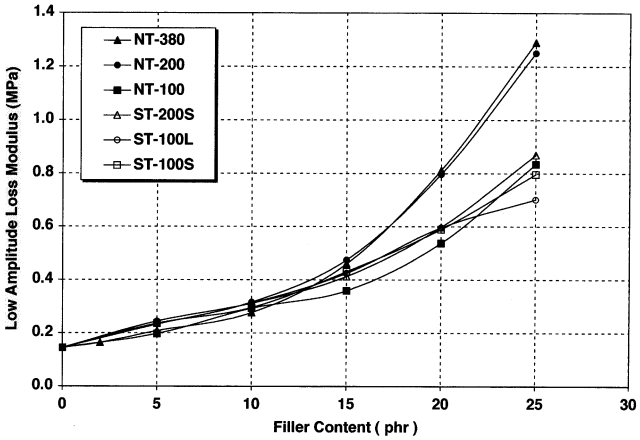

Figure 5. LALM vs filler content at 90 °C and 5 Hz for 83K PVAc composites of all silica fillers.

slightly filler dependent and located roughly between 12 and 15 phr (6−7.5 vol %). Above this range, the LAM rises very rapidly with filler addition. This behavior is also seen in filled elastomers. The Guth−Gold equation is included in Figure 4 and grossly underestimates the LAM values at all filler concentrations. Fillers NT-380 and NT-200 provide nearly identical reinforcement (that is, increase in the LAM) at all filler concentrations and ST-100S the poorest reinforcement. For the 100 series composites at 25 phr filler concentration, the LAM values are in the order ST-100L > NT-100 > ST-100S, indicating a strong dependence on surface treatment. Similarly, the reinforcement of ST-200S is much lower than NT-200, notwithstanding that both fillers have comparable sizes. The low reinforcement of NT100 compared to that of NT200 and NT380 suggests a possible size effect but may also be indicative of some filler agglomeration, as discussed later.

The effects of filler addition on the LALM are shown in Figure 5. The loss modulus also increases nonlinearly with filler concentration around 12 phr (6 vol %). While similar in appearance to Figure 4, there are substantial differences in the enhancement of the loss modulus relative to that of the storage modulus. Once again, NT-380 and NT-200 composites show the largest increases in moduli. The variations of loss moduli among the remaining fillers are minor and substantially lower than the corresponding variations in storage moduli shown in Figure 4.

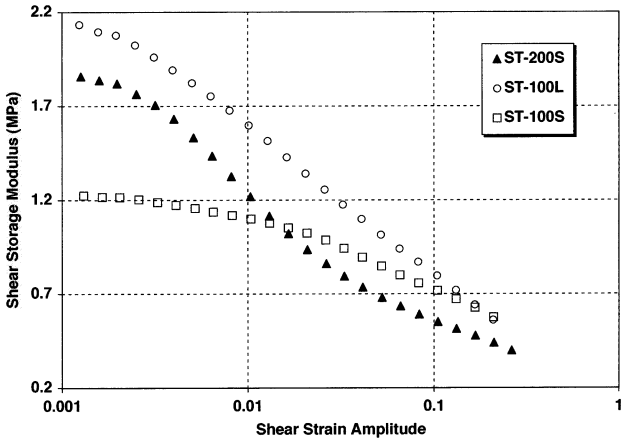

Figure 6. Shear storage modulus vs shear strain at 90 °C and 5 Hz for 25 phr 83K PVAc composites of all ST silica fillers.

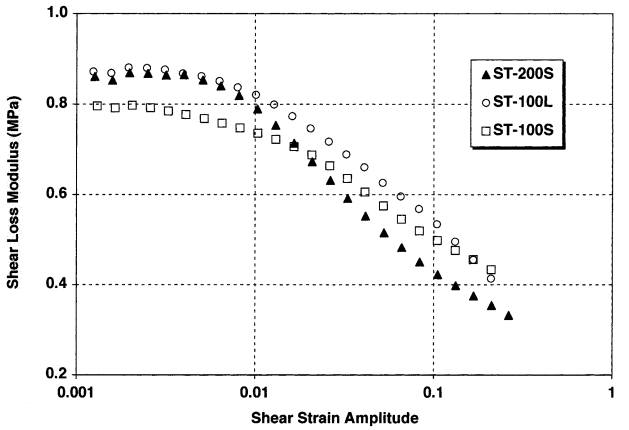

Figure 7. Shear loss modulus vs shear strain at 90 °C and 5 Hz for 25 phr 83K PVAc composites of all ST silica fillers.

While all filler types display qualitatively similar behavior to what is shown in Figures 1 and 2, surface treatment has a major effect on the relative rates at which the storage and loss moduli decrease with strain amplitude. NT composites all behave similarly as will be shown later, but the ST composites each behave uniquely, as shown in Figures 6 and 7 for the storage and loss moduli, respectively, at the 25 phr filler concentration. ST-100L and ST-100S composites show a large difference in LAM but converge at higher strain amplitudes (Figure 6), suggesting a similar reinforcement mechanism at high strains. ST-200S composite has a falloff rate in the mid-strain region (0.03 strain) that is appreciably higher than the other ST composites. Comparing Figure 6 to Figure 1 (which is typical of all NT composites), the NT composites appear to approach a limiting value of the LAM, whereas the ST composites do not. This behavior at low strains is discussed in more detail later. The reduction of loss modulus is shown in Figure 7, and it is obvious that the differences (in both magnitude and falloff rate) among the ST composites are minimal when compared to the differences for the storage moduli shown in Figure 6. Thus, a particular filler surface treatment affects storage and loss moduli differently, and this is most clearly illustrated by comparing the loss factors (ratio of loss modulus to storage modulus) for the various composites.

The loss factors for the neat polymer and for composites of the untreated fillers at 25 phr concentration are shown in Figure 8. All NT composites show nearly

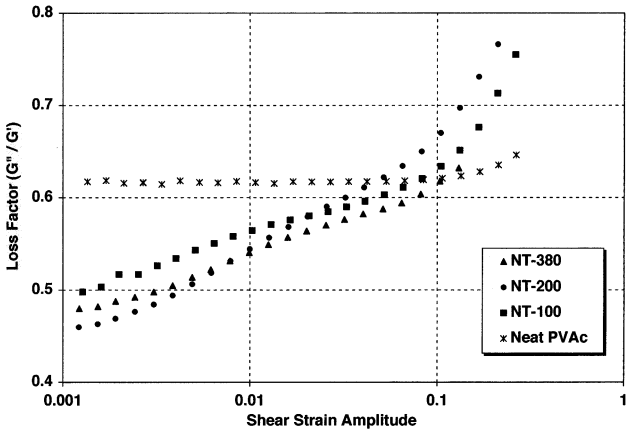

Figure 8. Loss factor vs shear strain at 90 °C and 5 Hz for 25 phr 83K PVAc composites of all NT silica fillers. Data for neat 83K PVAc are also shown.

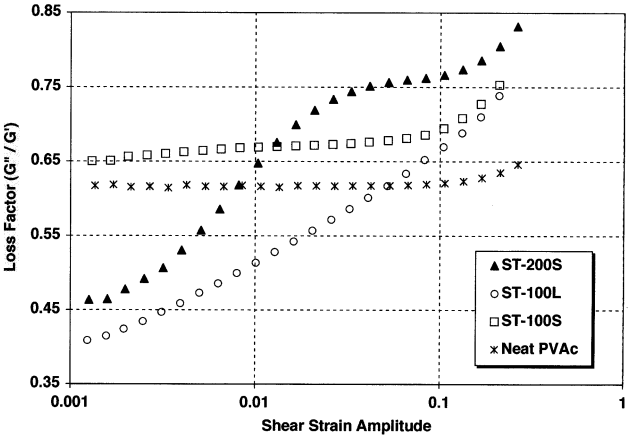

Figure 9. Loss factor vs shear strain at 90 °C and 5 Hz for 25 phr 83K PVAc composites of all ST silica fillers. Data for neat 83K PVAc are also shown.

identical behavior with strain amplitude. Thus, while NT-100 filler provides very poor reinforcement in composites, its effects on the values of loss factor and its changes with strain are nearly the same as for the highly reinforcing NT-200 and NT-380 fillers. At low strains, the loss factors of the NT composites are substantially lower than that of the neat polymer, while at higher strains the reverse is true. Note that at strain amplitudes above 0.1 the loss factor for the neat polymer also increases with strain, but at a lower rate than for the NT composites.

The situation is more complicated for the surface-treated fillers. Loss factors for all ST filler composites at 25 phr filler concentration are shown in Figure 9. The ST-100S composite has a loss factor vs strain curve that is nearly flat until about 0.1 strain and similar to the behavior of the neat polymer. However, in distinction to the neat polymer, the ST-100S composite is nonlinear at all strains, the constant loss factor merely reflecting the proportional decrease of storage and loss moduli at strain levels below 0.1. This composite is the only one to have a loss factor that is higher than that of the neat polymer at all strains, indicating a greater effect of the filler on the loss modulus than on the storage modulus, even at low strains.

The ST-200S composite (Figure 9) has a substantially reduced loss factor at low strains relative to that of the neat polymer and displays a loss factor that increases with strain amplitude beginning at strains as low as

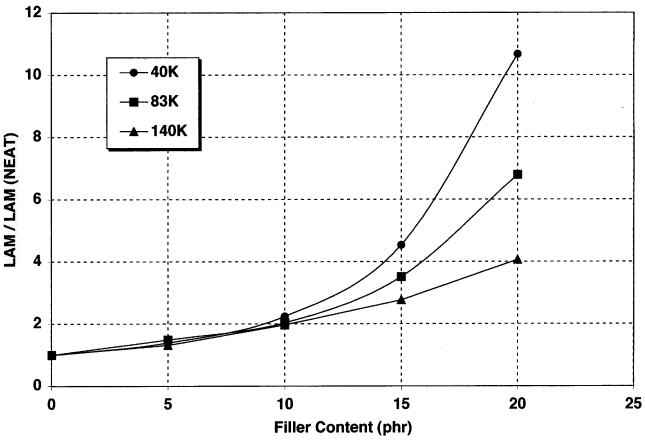

Figure 10. Relative reinforcement at low strain (LAM of the composite divided by the LAM of the neat polymer) vs filler content for PVAc of three molecular weights filled with NT-380 silica at 90 °C and 5 Hz.

0.002. Note the appearance of a "plateau" in the loss factor with a value of about 0.75 beginning at about 0.03 strain, which is higher than the loss factor for the neat polymer (ca. 0.61) or any other composite at the same strain. At low strains, however, the ST-200S composite has a loss factor that is nearly the same as that of the NT composites (Figure 8).

The ST-100L filler is special in that it contains tethered silicone chains. At low strains, the composite with this filler (Figure 9) displays a loss factor (ca. 0.40) that is lower than that of the neat polymer or any other composite. Thus, while ST-100L filler does not give the most effective reinforcement (Figure 4), it provides a larger increase in LAM relative to the increase in LALM than any other filler. In addition, the loss factors for ST-100L composites display a nearly constant rate of increase with strain amplitude, and there is no linear region. All ST filled composites converge to similar behavior and values of the loss factor at high strains, notwithstanding their dramatic differences at low strains.

The preceding results are all on composites with the 83K PVAc matrix polymer. The effect of matrix molecular weight on relative reinforcement (LAM of the composite relative to the LAM of the neat polymer) is shown in Figure 10 for the NT-380 composites. For filler concentrations below ca. 10 phr, the relative reinforcement is linear with filler content and nearly independent of molecular weight. Above ca. 10 phr, the relative reinforcement is highly nonlinear with filler content and strongly dependent on molecular weight. The highest relative reinforcement occurs with the lowest molecular weight matrix. However, this is in the reverse order of the actual LAM values, the lowest LAM being obtained at the lowest molecular weight. Identical results are obtained for all filler-type composites.

The effects of matrix molecular weight on the loss factor vs strain behavior for the ST-100S and ST-200S composites are shown in Figure 11, and the NT-380 and ST-100L composites are shown in Figure 12. The composites are compared at 20 phr filler concentration, since it was difficult to obtain a good dispersion of fillers in the 140K MW matrix at higher concentrations, and higher filler concentrations also produced composites that were too stiff for high strain measurements when using the same test fixture. While all loss factor curves retain their characteristic shapes at all molecular weights, the range of loss factor values from low to high

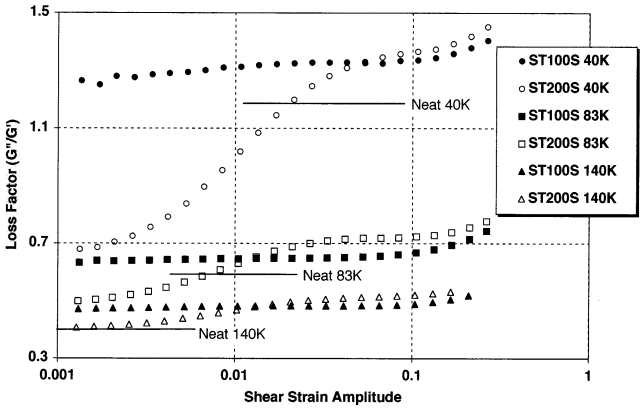

Figure 11. Loss factor vs shear strain for PVAc of three molecular weights filled with ST-200S silica or ST-100S silica at 20 phr, 90 °C, and 5 Hz. The nearly constant loss factor values for neat 40K, 83K, and 140K PVAc are indicated for comparison.

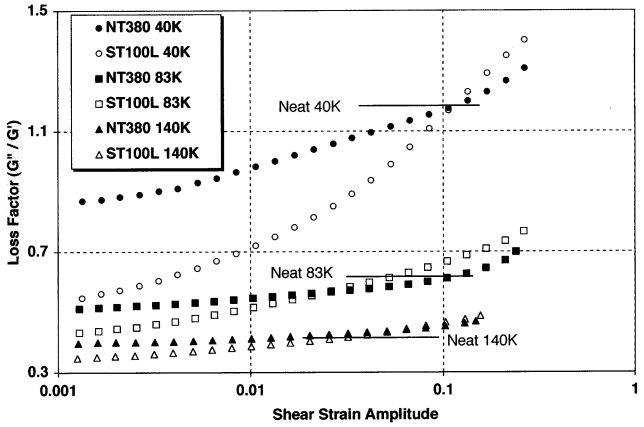

Figure 12. Loss factor vs shear strain for PVAc of three molecular weights filled with NT-380 silica or ST-100L silica at 20 phr, 90 °C, and 5 Hz. The nearly constant loss factor values for neat 40K, 83K, and 140K PVAc are indicated for comparison.

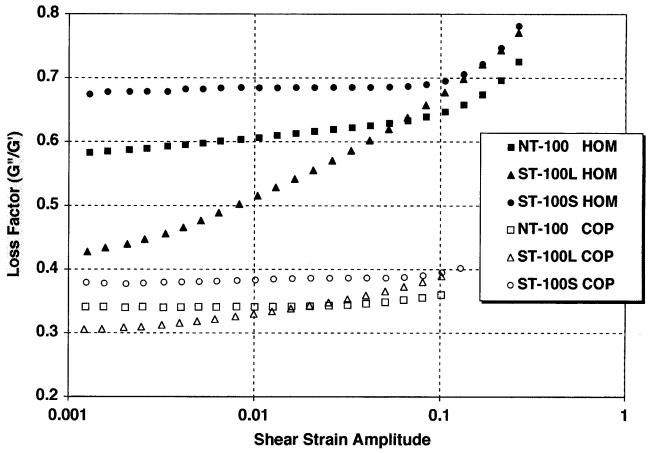

Figure 13. Loss factor vs shear strain amplitude for 83K PVAc (HOM) and 92K PVAC−PVOH copolymer (COP) filled with NT-100, ST-100L, or ST-100S silica at 20 phr, 95 °C, and 5 Hz.

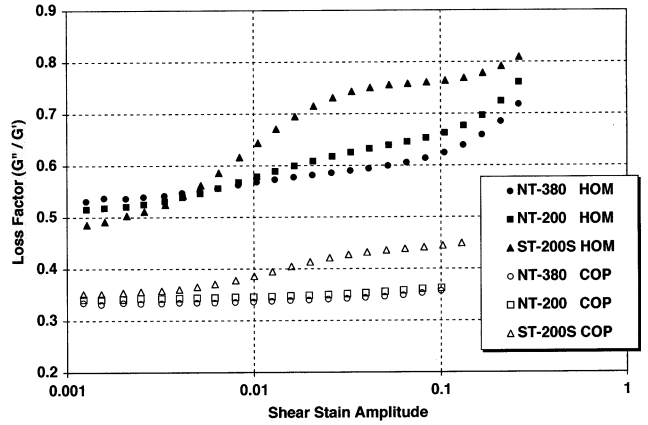

Figure 14. Loss factor vs shear strain amplitude for 83K PVAc (HOM) and 92K PVAC−PVOH copolymer (COP) filled with NT-380, NT-200, or ST-200S silica at 20 phr, 95 °C, and 5 Hz.

strains is dramatically lowered by an increase in matrix MW. With the 140K MW matrix, the loss factors are nearly constant with strain and almost independent of filler surface treatment. Thus, higher molecular weight matrices lead to more similar behavior of the composite storage and loss moduli with strain, a greatly reduced effect of filler surface treatment on composite behavior, a much lower degree of nonlinearity in the loss factor, and lower relative reinforcement by filler addition.

The importance of the matrix phase in determining the properties of the composite is clearly illustrated by the previous results on matrix molecular weight. Another means by which to alter the effectiveness of the matrix in transferring strain (or stress) to the filler interface is to use a copolymer such as PVAc−PVOH. This copolymer can act as both a proton donor and acceptor, and thus can form hydrogen bonds within and among the chains, as well as with the untreated silica−filler surfaces. Recall that the homopolymer PVAc can only accept hydrogen bonds, such as from surface hydroxyls on the NT fillers. Thus, the copolymer chains should exhibit the characteristics of enhanced entanglement density, as compared to the homopolymer of the same molecular weight. The loss factor behaviors of the (83K MW) homopolymer and (92K MW, with 18% OH) copolymer composites with NT-100, ST-100L, and ST-100S fillers at 20 phr are given in Figure 13, and the composites with the NT-380, NT-200, and ST-200S fillers are given in Figure 14. The copolymer effect completely mimics the effect of a higher MW matrix, showing both a lower range of nonlinearity and greatly reduced dependence on filler type when compared to the behavior of the composites with the homopolymer matrix.

The present experimental results demonstrate that the reinforcement and nonlinearity are strongly dependent on the filler surface treatment. Additionally, the effects of molecular weight for the homopolymer matrix and hydrogen-bonding copolymer substitution for the homopolymer strongly suggest that the root origins of the reinforcement and nonlinear behavior reside in the polymeric matrix. Filler particle size also plays a key role. It is our belief that the filler−polymer interactions result in a change in the entanglement (density and distribution) state of the matrix that is responsible for the high reinforcement levels observed at low strains. Breakdown of this modified entanglement state is postulated to cause the reduction of storage and loss moduli with increasing strain levels, and correspondingly the restoration of the modified state is believed to be responsible for the recovery of moduli following large strain perturbations.[32]

Chain Conformation, Trapped Entanglements, and the Langevin Effect

In this study, all interfacial bonding between filler particles and the matrix is labile, ranging from physical adsorption (ST-100S and ST-200S fillers) to hydrogen bonding (NT series fillers) to the interpenetration of surface-tethered and matrix chains (ST-100L). These labile bonds result in a partial immobilization of the matrix chains that will be referred to as "trapped entanglements". Chains may have multiple bonding contacts with the filler, thereby resulting in chain loops that are substantially shorter than the overall chain. It is easily shown that for PVAc of 83K MW about seven mers per cubic nanometer are required to obtain the bulk density. On the basis of the nearly Gaussian distribution of chain segments from a chain's center of mass, it can be shown that a single chain contributes at most 7% of the segments required to fill space. Thus, the interpenetration of the statistical domains of many polymer chains is a given. Clearly, this "statistical intimacy" leads to some degree of influence of the deformation of one chain coil on another, and the entanglement concept is one way to view this mutual interaction among chains.

The trapped entanglements of chains having direct contact with the filler surface must therefore influence the far-field mobility of other chains. It is expected that high strain amplitudes would enhance the kinetics of chain debonding (or slipping) at the surface and lead to added mobility and lower dynamic stiffness of the matrix phase overall. The release of trapped entanglements at the filler surface leads to a reduction of the composite modulus, a micromechanical effect dependent on the boundary conditions describing the polymer−filler coupling. For example, a commonly used boundary condition for solids is that of displacement (elastic) continuity at the interface. For liquids, the commonly used condition is that of velocity (no slip or viscous) continuity at the interface. There are other possibilities, for example, the compliant interface proposed by Hashin,[33] and these lead to different degrees of reinforcement. Similarly, a change in boundary condition from no-slip to slip at the interface would itself reduce the reinforcement of the composite. However, a second mechanism rooted in the statistical theory of chain conformation is also enabled by slippage at the interface, and this leads to a greater reduction in composite modulus than would be expected solely from the micromechanical considerations of two phases of constant component moduli but variable phase coupling.

From the thermodynamic theory of polymers it is known that the chains in a melt are essentially unperturbed in dimensions (the well-known Flory concept that a melt is its own Θ solvent). Gaussian chain statistics are most commonly used to describe the end-to-end distance of chains in the melt. Straightforward statistical arguments lead to the well-known result that a freely jointed, freely rotating Gaussian chain will exhibit an entropic restoring force given by $f = 3kTr/nl^2$. In this equation, k is Boltzmann's constant, T is absolute temperature, r is the end-to-end distance, n is the number of links in the chain, and l is the length of a link. The Gaussian chain is always Hookean but is not applicable for values of relative chain extension (r/nl) approaching unity, in which case the chain obeys Langevin, not Gaussian, statistics. Then the entropic restoring force in dimensionless form is more accurately given by $fl/kT = L^*(r/nl)$, where L^* is the inverse Langevin function.[34] For values of relative chain extension (r/nl) approaching zero, the inverse Langevin function approaches $3(r/nl)$, and the chain exhibits the same stiffness as does a Gaussian chain.

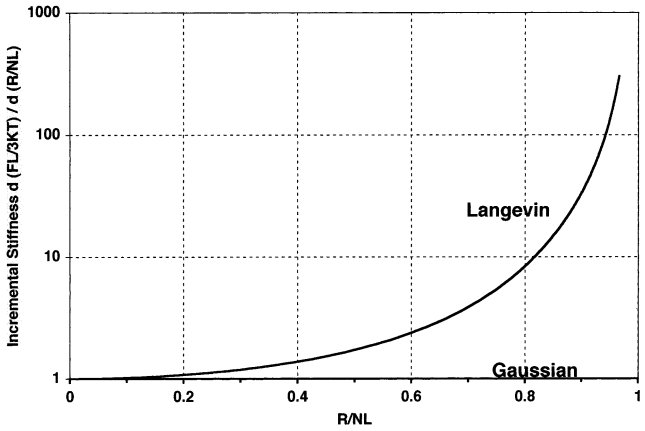

Figure 15. Incremental chain stiffness, expressed as the normalized slope of the Langevin function, vs relative extension r/nl. The incremental stiffness for a Gaussian chain is always unity on this graph.

Table 2. Langevin Chain Compared to the Gaussian Chain at Intermediate Relative Chain Extensions[a]

r/nl	$fl/3kT$ (Langevin)	force ratio (Langevin/Gaussian)	$d(fl/3kT)/d(r/nl)$ (Langevin)
0.313	0.333	1.064	1.21
0.438	0.500	1.142	1.49
0.537	0.667	1.242	1.92

[a] Note that the first column also represents the Gaussian force prediction for $fl/3kT$ as well as r/nl.

For reasons to be discussed shortly, the deviations from Gaussian (Hookean) behavior are larger than generally recognized, as indicated by the incremental stiffness (or normalized slope) of the Langevin chain, namely $d(fl/3kT)/d(r/nl)$, which is the derivative of the inverse Langevin function divided by three. The incremental stiffness is shown in Figure 15, and it is apparent that deviations from Hookean behavior are displayed at relative chain extensions (r/nl) as low as 0.2. Bear in mind that the incremental stiffness as defined here is unity for a Gaussian chain at all values of (r/nl). The Langevin chain becomes stiffer rapidly as (r/nl) increases. Therefore, a shorter chain (lower n) will be stiffer than a longer chain with the same end-to-end distance r. Since Figure 15 is difficult to read at low values of (r/nl), we include Table 2, which gives some values for the force and incremental stiffness of the Langevin chain relative to those of the Gaussian chain. Note that, for a chain with a relative extension of 0.438, the force generated is 14% higher than for a Gaussian chain but that the incremental stiffness is already 49% higher than the Hookean behavior. The high incremental stiffness may be relevant to the appearance of a "bound" polymer layer of finite thickness that some authors postulate exists at the filler−matrix interface. In our view this layer is a region exhibiting short chain Langevin statistics. Energetic (bonding) interactions with the filler surface are limited to the chains in immediate contact with the surface, with the far-field effects due to entanglement coupling. The gradient of entanglement density in the region surrounding a filler particle is a crucial but as yet unresolved issue in polymer physics. Hence, the matrix modulus as a

function of distance from the filler surface is also unknown.

The incremental stiffness of the Langevin chain (Figure 15) may be far more important to the behavior of filled elastomers than previously considered for yet another reason that is somewhat obscure and which we will refer to as "reference state bias". In the simplest terms, the chains of a polymer network, such as either a cross-linked elastomer or an entangled polymer melt, in its reference configuration (i.e., the undeformed state of the macroscopic sample), obviously have a distribution of end-to-end distances. Clearly, all chains do not have an (r/nl) value of zero, and we label the relative extension of a chain in this reference state as $(r/nl)_0$. But according to either Gaussian or Langevin statistics, such a chain exerts a restoring force. What is the reaction to this reference state force if the material is undeformed and therefore externally stress-free?

If one examines the early work on rubber elasticity,[34] it is clear that the nonzero forces exerted by the chains in the reference state give rise to an internal isotropic stress that tends to change the density of the material but is resisted by the high bulk modulus. Thus, the conformational entropy associated with the nonzero values of (r/nl) for the assembly of chains becomes part of the material's reference-state free energy. If an external deformation is now imposed on the material, then each chain will undergo a change in relative extension, namely $(r/nl) - (r/nl)_0$. This leads to deviatoric deformations only that are resisted by the shear modulus, which for a soft material (e.g., polymers above the glass transition temperature) is many orders of magnitude lower than the bulk modulus. Thus, insofar as each chain is concerned, it is being deformed relative to its reference state deformation. For Gaussian networks this is irrelevant since all chains are always Hookean. However, for a Langevin chain the reference state determines its incremental response stiffness. Thus, referring to Table 2, a chain with a "bias" or reference state extension of 0.438 begins with a stiffness that is already 49% higher than expected from the Gaussian theory. In filled systems, filler-trapped entanglements result in more subchains with larger nonzero bias $(r/nl)_0$, further enhancing the effect of incremental chain stiffness. It follows that the incremental stiffness (Figure 15) is more relevant to the behavior of filled polymers than the integral force−deformation curve itself.

The effectiveness of a particular filler to produce trapped entanglements will depend on its surface treatment, specific surface area, and volume fraction. The effect of surface chemical treatment will be discussed in detail later. To illustrate the latter two variables, consider a simple cubic unit cell model in which the filler particles are all of equal size with a diameter of D. It is easily shown that the ratio of the particle surface-to-surface spacing S (measured along the axes of the unit cell) divided by the particle diameter is given by

$$\frac{S}{D} = \frac{1 - 2X}{2X}$$

$$\text{where } X = \left(\frac{3\phi}{4\pi}\right)^{1/3} \text{ and } \phi = \text{vol fraction filler}$$

The ratio S/D is shown in Figure 16 as a function of filler volume fraction. Note that at the relatively low filler concentration of about 6.5 vol % the ratio S/D passes through unity. Thus, if the particles have, for example, a diameter of 20 nm, then the particles have an average spacing (surface-to-surface) of 20 nm as well. For the 83K MW PVAc used in this study, the polymer molecule's radius of gyration is about 20 nm.

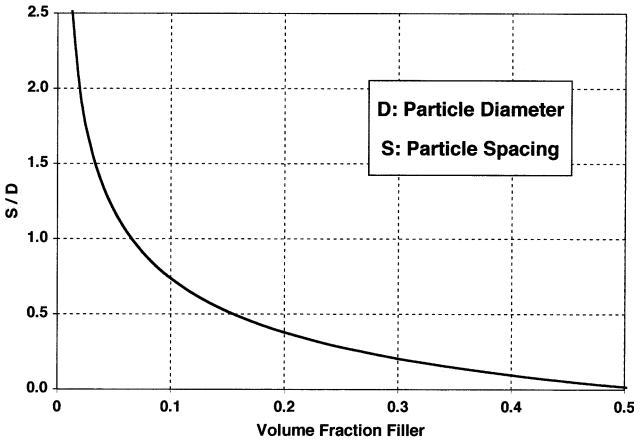

Figure 16. Ratio of surface-to-surface particle spacing (S) to the particle diameter (D) vs volume fraction of filler for a simple cubic lattice model.

Notwithstanding the complications associated with some agglomeration that is always present, the particle spacing and size calculations demonstrate the plausibility that the nanoscale particles are able to significantly alter the mobility and conformational freedom of both the near- and far-field matrix chains. The interactions at the filler surface lead to a trapped entanglement zone or boundary layer around each filler particle, regardless of particle size. However, smaller particles will have a greater surface area, and consequently the boundary layer material encompasses a greater fraction of the matrix. Moreover, the interparticle spacing is also small enough so that there is a finite probability that some chains are influenced by more than one particle, a "bridging effect" or overlapping of boundary layers. This bridging may be responsible for the nonlinearity of reinforcement vs filler concentration shown in Figures 4 and 10 around 12 phr (6 vol %). We speculate that the differences in behavior of storage and loss moduli with filler content (Figures 4 and 5) may be due to the relative effects of the boundary layer and the bridging as related to the filler surface treatment. Clearly, storage modulus would be predominantly affected by bridging while loss modulus would be more dependent on boundary layer formation. The two phenomena cannot truly be separated, but it is advantageous to visualize them as separate mechanisms.

Thus, trapped entanglements and chain loops resulting from polymer−filler bonding give rise to a subset of stiffer chains extending from the interface, resulting in a dynamically stiffer matrix as well as a higher loss modulus due to an increase in hydrodynamic friction (or boundary layer thickness). The LAM value of the composite is consequently higher than would be expected from conventional micromechanical considerations. As the trapped entanglements are relaxed due to an applied external strain (or stress), the subset of short chains will disappear and the matrix will be composed of longer chains that, on average, display more Gaussian behavior. From Figure 15, lower incremental stiffness of the matrix results from the reduced bias. Calculations pertaining to the effects of Langevin chain statistics on matrix stiffness as a function of filler

size and concentration are in progress and will be reported in the future.

Discussion

The substantial differences in reinforcement (LAM values) among the composites of all six fillers are clearly related to the filler surface area (or filler size) and surface treatment as shown in Figure 4. The existence of a "filler size effect" is consistent with the calculations on the interparticle distances and associated boundary layers and bridging effects. However, filler agglomeration may tend to obscure the effect of particle size. Although all fillers are well dispersed even at the highest concentrations, some agglomeration may still occur. During sample preparation, it was observed that the NT fillers were generally more difficult to mix with the polymer than the ST fillers and that the ST-100S was the most difficult to mix in the ST filler series.

The role of surface treatment is clearly shown when comparing composites of fillers with the same size. From the LAM values at 25 phr filler content shown in Figure 4, the reinforcement capability for the 200 series fillers is in the order NT-200 > ST-200S and for the simple (nonpolymeric) 100 series fillers is NT-100 > ST-100S. For both filler sizes, the NT fillers provide a more effective reinforcement than the simple ST fillers due to the formation of hydrogen bonds with the matrix polymer. However, in the case of the ST-100L filler, the reinforcement is the highest among the 100 series fillers and also higher than the ST-200S filler. This high reinforcement capability is attributed to the surface-tethered polymer chains that are well mixed with the matrix chains, resulting in a more extensive boundary zone. Evidence for this chain mixing has been found in the broadening of the loss modulus dispersion around the T_g of the host polymer.[31] The broadening, which is unique to the ST-100L composites, is found to occur on the low-temperature side of the T_g dispersion (at constant frequency), indicating that there is added mobility relative to that of the unfilled polymer. The surface-tethered silicone polymer chains have a much lower T_g than the matrix PVAc and therefore provide additional free volume in a mixture with the matrix polymer.

The characteristics of individual fillers are best delineated by their loss factor behavior. Despite their different levels of reinforcement, all NT fillers give very similar loss factor curves as shown in Figure 8, due to similar nonlinear behavior of their storage and loss moduli with strain. It appears that the differences in reinforcement are primarily due to the particle size, with the surface properties governing the characteristics of the nonlinear viscoelasticity. If agglomeration does exist, it is most likely different for different filler sizes. Their common nonlinear loss factor behavior with strain implies that the nonlinearity is not caused by deagglomeration.

The loss factor curves for all ST composites are dramatically different as seen in Figure 9 and are the result of the differences in relative behavior of the component moduli for each composite as seen in Figures 6 and 7. The loss factor of the ST-100S composite, which is nearly constant and always higher than the loss factor of the neat polymer at all strains, indicates a behavior that is similar to the effect of filler addition to a simple viscous liquid. Viscous coupling of the filler to the matrix and the usual hydrodynamic boundary layer effect result in an increase in viscosity. In terms of the proposed mechanism, the boundary layer formation is sufficiently weak (low trapped entanglement density) that bridging is nearly nonexistent, as indicated by the low reinforcement capability for this filler. This results in the proportional reduction of storage and loss moduli with strain and therefore the constancy of the loss factor.

The behavior for the ST-200S composite (Figure 9) is attributed to the easy "peeling" of host polymer from the surface at low strains (below 0.03). The loss factor behavior thereafter (above 0.03 strain) is governed by the boundary layer effect, resulting in a plateau that is similar to the ST-100S composite behavior and indicative of a loss of bridging. It is conjectured that the ST-200S composite displays the characteristics of the three viscous boundary layer regimes described by Leger et al.[22] for unfilled polymer flow over a flat surface. For the ST-100L composite, its nearly constant rate of increase of loss factor with strain (Figure 9) is attributed to the continuous decoupling or disentanglement between surface-tethered chains and the matrix chains. However, the interfacial "bonding" can sustain higher strains due to its higher strength when compared to the ST-200S filler. Stated differently, it is expected that the disentanglement of surface-tethered and matrix chains (ST-100L) requires more work than does the peeling of chain segments in direct contact with a simple ST filler surface (ST-200S).

All ST filler surfaces show viscous coupling with the matrix at all strains. In contrast, the storage modulus for the NT-380 composites tends to plateau or level out at lower strains as shown in Figure 1. This implies a region of "elastic coupling", which is similar to a "composite effect" in which filler of higher modulus is elastically coupled to a matrix of lower modulus. However, the distinction between elastic and viscous coupling is somewhat arbitrary since all filler interactions, whether elastic or viscous, will result in trapped entanglements of matrix chains, and all composites display the attributes of viscous coupling with increasing strain upon the release of these trapped entanglements. The distinction is purely a question of the storage modulus behavior at limiting small strains. Additional studies using substantially lower strain amplitudes (below 0.001) are needed to resolve the issue of whether there is a true low strain limit for elastic coupling.

It is noted that all filled polymers as well as the neat polymer (Figures 8 and 9) show an upturn in the loss factor at strains greater than 0.1. The upturn in the loss factor for the neat polymer is due to disentanglement of the chains, which results in lower storage and loss moduli, but with a higher relative reduction in the storage modulus. This ultimately manifests itself in the behavior of the filled systems since overall composite stiffness (absolute value of the complex modulus) governs the ability to transmit far-field stresses through the matrix to the filler surface, which in turn enables the disentanglement process. For a given bond strength, a more compliant matrix would result in a lower debonding rate at any given far-field strain. Moreover, filler addition results in a greater increase in the LAM than in the LALM (Figures 4 and 5), except for the ST-100S filler, and this results in a greater potential for reduction in storage modulus and hence an upturn in loss factor at high strains.

Table 3. Effect of Matrix Molecular Weight on the Composite LAM and HAM for All Fillers at 20 phr Concentration[a]

filler	MW	LAM (0.002)	HAM (0.10)	HAM/LAM
NT-380	140K	1.52	1.10	0.724
	83K	1.57	0.778	0.496
	40K	0.638	0.248	0.389
NT-200	140K	1.44	0.914	0.635
	83K	1.65	0.675	0.409
	40K	0.592	0.143	0.242
NT-100	140K	1.24	0.778	0.627
	83K	1.03	0.557	0.524
	40K	0.354	0.125	0.353
ST-100L	140K	1.69	1.0	0.592
	83K	1.36	0.611	0.449
	40K	0.621	0.196	0.316
ST-200S	140K	1.52	0.868	0.571
	83K	1.20	0.424	0.353
	40K	0.701	0.152	0.217
ST-100S	140K	0.933	0.760	0.815
	83K	0.924	0.615	0.666
	40K	0.256	0.160	0.625

[a] Moduli are in MPa; the LAM was measured at 0.002 strain and the nonterminal HAM at 0.10 strain.

The slopes of loss factor vs strain (above 0.1) for the filled systems are in the order NT > ST > neat polymer. For the NT series composites (Figure 8), hydrogen bonds between the filler surface and the host polymer provide added frictional or drag forces, thereby lessening the rate of reduction in loss modulus. Stated differently, the NT fillers provide a higher "viscous" boundary layer radius than the ST fillers at all strain levels. Thus, the hydrogen bonding that is believed responsible for the appearance of elastic coupling at small strains also persists in influencing the high strain behavior. The ST composites (Figure 9) all approach similar behavior at high strains, which suggests that once entanglement trapping at the filler surface is overcome, these fillers exhibit very similar frictional interactions with the matrix. However, this common value of frictional interaction is lower than that in the NT composites, as expected. These concepts obtain additional support from the influence of matrix molecular weight and copolymer composition on the viscoelastic properties.

A summary is given in Table 3 for the composite LAM and HAM values obtained with the various molecular weight matrices and with a filler concentration of 20 phr. Higher molecular weights result in larger LAM and HAM values, but with a greater increase in the HAM. Thus, the HAM/LAM ratio increases (toward unity) with increasing matrix molecular weight. This is most clearly shown in the loss factor behavior (Figures 11 and 12). The primary reason for the reduced effect of strain on loss factor at higher matrix molecular weights is the higher HAM/LAM ratio. The low MW 40K matrix accentuates the role that the filler interface has on composite properties since the neat polymer has the lowest entanglement density to start with. Consequently, any reinforcement (Figure 10) due to trapping of entanglements at the filler−matrix interface, or the subsequent release under stress of these entanglements, will be dramatic and represent a disproportionate perturbation to the entanglement density, thereby causing the extensive nonlinear viscoelastic behavior that is shown in Figures 11 and 12. Conversely, as the matrix MW increases, so does the native entanglement density, and there is less relative effect resulting from the trapping of entanglements by the filler or their subsequent release under stress. There is no obvious or compelling reason to invoke filler agglomeration arguments.

For each MW polymer, comparison of the filled systems with the neat polymer shows that the (crossover) strain at which the loss factor of the filled material exceeds that of the neat polymer decreases substantially as the MW increases. For the NT-380 and ST-100L fillers (Figure 12) with 40K matrix, the crossover occurs above 0.10 strain, whereas the crossover is about 0.03 strain for the 140K MW matrix. Similarly, for the ST-200S (Figure 11) with 40K matrix, the crossover is about 0.02 strain while for 140K matrix it is about 0.002 strain. ST-100S always exhibits a loss factor that is higher than that of the neat matrix and so this filler has a crossover strain less than 0.001 if it exists at all. Higher MW matrices can more efficiently transfer external strains to the internal filler surfaces and thus give lower crossover strains for any particular filler surface treatment. Conversely, for a given MW matrix, those fillers that provide the highest reinforcement, such as NT-380 and ST-100L, also give higher crossover strains than do the lower reinforcement fillers such as ST-100S and ST-200S. More effective interfacial bonding leads to both higher reinforcement and an increased strain threshold (at which the composite loss factor exceeds that of the neat polymer), as expected. Below the strain threshold the effect of filler addition renders the resulting composite more solidlike (lower loss factor than the neat polymer), while above the strain threshold the effect is to make the composite more viscous.

In the case of the copolymer matrix, the introduction of hydrogen bonding leads to a flattening of the loss factor curves and a lower dependence on the filler surface treatment for all filler types (Figures 13 and 14). That the copolymer has similar effects on the behavior of both NT and ST composites suggests again that the origins of the nonlinear behavior are rooted in the matrix and the filler−matrix bonding. It would be difficult and challenging to explain the results of molecular weight changes or copolymer substitution in terms of a filler agglomeration theory. It is our opinion that the concept of entanglement trapping of matrix chains at filler surfaces, and the manner in which strain releases these trapped entanglements, is a more plausible explanation for the nonlinear viscoelastic behavior of filled polymer melts and elastomers.

Any viable theory for the mechanism of nonlinear viscoelasticity in filled polymers must correspondingly explain the restoration of moduli following a destructive reduction by a large strain perturbation. Preliminary moduli recovery experiments are completely consistent with the mechanism proposed here and have been submitted for publication elsewhere.[32]

Conclusions

Mechanisms governing the nonlinear viscoelasticity of nanofilled polymer melts have been explored in the present work. Filler size, concentration and surface chemistry, and the entanglement characteristics of the matrix polymer appear to be the primary factors determining both the high reinforcement and concomitant nonlinear viscoelasticity. Simple scaling calculations show that nanofillers at relatively low concentrations provide a high level of interfacial area for polymer−filler interactions and that the particle spacing and size are both of comparable dimensions to a macromolecular coil. Contributions from filler structure may exist as well but

seem to be minor. The low concentrations of filler make the presence of a large-scale filler network (percolation) unlikely, and evidence from SEM observations and visual examinations (the transparency of the samples) confirms this and the limited agglomeration. Therefore, filler structure and networking that are often present for high filler concentration composites are not major factors in the present study.

The effects of filler surface treatment, molecular weight of the matrix, and substitution of a hydrogen-bonding copolymer for the homopolymer matrix all indicate strongly that the entanglement structure in the matrix is the dominant factor in determining the viscoelastic behavior of the composite. Trapping of polymer chain loops at the filler surface results in a higher entanglement density, and a gradient of this density with distance from the filler surface, which is related to the surface treatment of the filler and its interactions with the matrix polymer. Non-Gaussian (Langevin) chain statistics associated with shorter chain segments become important in the presence of filler and greatly enhance the storage and loss moduli of the composite above those that are predicted by simple micromechanical mixing models.

The loss of trapped entanglements resulting from the stress (or strain)-induced debonding of chain segments from the filler surface facilitates the relaxation of the matrix entanglement structure, resulting in the observed viscoelastic nonlinearity. In this regard, the process is conceptually similar to what is known to occur in the flow of unfilled polymers over flat surfaces. Similarities in the present results to previous work on filled elastomers suggest that the mechanism governing the reinforcement and nonlinearity in filled cross-linked systems may be the same as postulated here for filled un-cross-linked melts. Filled elastomers used in engineering applications typically have much higher filler concentrations than examined here. Nevertheless, the nonlinear behavior associated with trapped entanglements should be considered to be as relevant as any nonlinear behavior associated with filler agglomeration phenomena.

Acknowledgment. The authors are grateful to the National Science Foundation (CTS-9871894) and Office of Naval Research (N00014-99-1-0187) for their generous support of this research at its inception and to ONR for its continuing support (N00014-01-0732). Thanks are also due to the Cabot Corp. for generously supplying the fillers used in this investigation. We are also appreciative of the cooperative and complementary efforts by a number of our colleagues in this multiinvestigator program on the mechanisms of interaction of nanofillers with polymers. In particular, we acknowledge the interactions with Professors Keblinski, Picu, and Schadler and their graduate students, especially Benjamin Ash.

References and Notes

(1) Payne, A. R. *J. Appl. Polym. Sci.* **1962**, *6*, 57.
(2) Kraus, G. *J. Appl. Polym. Sci.: Appl. Polym. Symp.* **1984**, *39*, 75.
(3) Heinrich, G.; Kluppel, M. *Adv. Polym. Sci.* **2002**, *160*, 1.
(4) Maier, P. G.; Gortiz, D. *Kautsch. Gummi Kunstst.* **1996**, *49*, 18.
(5) Chazeau, L.; Brown, J.; Yanyo, L.; Sternstein, S. *Polym. Compos.* **2000**, *21*, 202.
(6) Faitelson, L. A. *Int. J. Polym. Mater.* **1980**, *8*, 207.
(7) Nielsen, L. E. *J. Compos. Mater.* **1967**, *1*, 100.
(8) Hsich, H. S. Y.; Hronas, M. J.; Hill, H. E.; Ambrose, R. J. *J. Mater. Sci.* **1984**, *19*, 2997.
(9) Ziegel, K. D.; Romanov, A. *J. Appl. Polym. Sci.* **1973**, *17*, 1119.
(10) Kraus, G. *Adv. Polym. Sci.* **1971**, *8*, 155.
(11) Wagner, M. P. *Rubber Chem. Technol.* **1976**, *49*, 703.
(12) Mills, N. J. *J. Appl. Polym. Sci.* **1971**, *15*, 2791.
(13) Kosinski, L. E.; Caruthers, J. M. *J. Non-Newtonian Fluid Mech.* **1985**, *17*, 69.
(14) Ziegelbaur, R. S.; Caruthers, J. M. *J. Non-Newtonian Fluid Mech.* **1985**, *17*, 45.
(15) Sobhanie, M.; Isayev, A. I.; Fan, X. *Rheol. Acta* **1997**, *36*, 66.
(16) Stauffer, D.; Aharony, A. *Introduction to Percolation Theory*; Taylor & Francis: London, 1992.
(17) Karasek, L.; Sumita, M. *J. Mater. Sci.* **1996**, *31*, 281.
(18) Gerspacher, M.; O'Farrell, C. P.; Tricot, C.; Nikiel, L.; Yang, H. H. Presented at the 150th Technical Meeting, Rubber Division, ACS, 1996.
(19) Payne, A. R. In *Reinforcement of Elastomers*; Kraus, G., Ed.; Interscience: New York, 1965.
(20) Wang, S. Q.; Inn, Y. W. *Rheol. Acta* **1994**, *33*, 108.
(21) Simhambhatla, M.; Leonov, A. I. *Rheol. Acta* **1995**, *34*, 329.
(22) Leger, L.; Raphael, E.; Henet, H. *Adv. Polym. Sci.* **1999**, *138*, 185.
(23) Yarin, A. L.; Graham, M. D. *J. Rheol.* **1998**, *42*, 1491.
(24) Bueche, F. In *Reinforcement of Elastomers*; Kraus, G., Ed.; Interscience: New York, 1965.
(25) Kosinski, L. E.; Caruthers, J. M. *Rheol. Acta* **1986**, *25*, 153.
(26) Isono, Y.; Nishitake, T. *Polymer* **1995**, *36*, 1635.
(27) Granick, S.; Hu, H. *Langmuir* **1994**, *10*, 3857.
(28) Peanasky, J.; Cai, L. L.; Granick, S. *Langmuir* **1994**, *10*, 3874.
(29) Granick, S.; Hu, H.; Carson, G. A. *Langmuir* **1994**, *10*, 3867.
(30) Shang, S. W.; Williams, J. W.; Soderholm, K.-J. M. *J. Mater. Sci.* **1994**, *29*, 2406.
(31) Zhu, A.; Sternstein, S. S. *Mater. Res. Soc. Symp. Proc.* **2001**, *661*, KK4.3.1.
(32) Zhu, A.; Sternstein, S. S. Nonlinear Viscoelasticity Of Nanofilled Polymers: Interfaces, Chain Statistics And Properties Recovery Kinetics. *Compos. Sci. Technol.*, in press.
(33) Hashin, Z. *J. Mech. Phys. Solids* **1991**, *39*, 745.
(34) Treloar, L. R. G. *The Physics of Rubber Elasticity*, 3rd ed., Clarendon Press: Oxford, 1975.

MA020482U